Supporting Information for:

DNA-Encoding to Improve Performance and Allow Parallel Evaluation of the Binding Characteristics of Multiple Antibodies in a Surface-Bound Immunoassay Format

*Adam L. Washburn, Joseph Gomez, Ryan C. Bailey**

Department of Chemistry, University of Illinois at Urbana-Champaign, 600 South Mathews Avenue, Urbana, Illinois 61801

*E-mail: baileyrc@illinois.edu

Table of Contents

Table S1. List of DNA oligonucleotide sequences used. All sequences have a 5′ terminal amino group attached via a 6-carbon chain (5AmMC6 from IDT)

Name	Sequence (5′ to 3′)
A	AAA AAA AAA AAT CCT GGA GCT AAG TCC GTA
A′	AAA AAA AAA ATA CGG ACT TAG CTC CAG GAT
B	AAA AAA AAA AGC CTC ATT GAA TCA TGC CTA
B′	AAA AAA AAA ATA GGC ATG ATT CAA TGA GGC
F	AAA AAA AAA AAT CAG GTA AGG TTC ACG GTA
F′	AAA AAA AAA ATA CCG TGA ACC TTA CCT GAT
K	AAA AAA AAA ATA ATC TAA TTC TGG TCG CGG
K′	AAA AAA AAA ACC GCG ACC AGA ATT AGA TTA
L	AAA AAA AAA AGT GAT TAA GTC TGC TTC GGC
L′	AAA AAA AAA AGC CGA AGC AGA CTT AAT CAC
M	AAA AAA AAA AGT CGA GGA TTC TGA ACC TGT
M′	AAA AAA AAA AAC AGG TTC AGA ATC CTC GAC

Table S2. List of DNA-antibody conjugates and the molar ratio of DNA to antibody as determined by UV-Vis measurements.

Conjugate Name	**DNA:Antibody Ratio**
B'-anti-PSA-B732M	0.4
L'-anti-PSA-B731M	0.4
M'-anti-PSA-5G6	0.9
B'-anti-AFP-B491M	0.6
L'-anti-AFP-210	0.5
M'-anti-AFP-301	0.9
A'-anti-PSA-8A6	0.4
K'-anti-PSA-Fitz	0.5
F'-anti-PSA-5A6	1.0
A'-anti-AFP-1301	1.5
K'-anti-AFP-1305	0.7
F3'-anti-AFP-Fitz	1.4

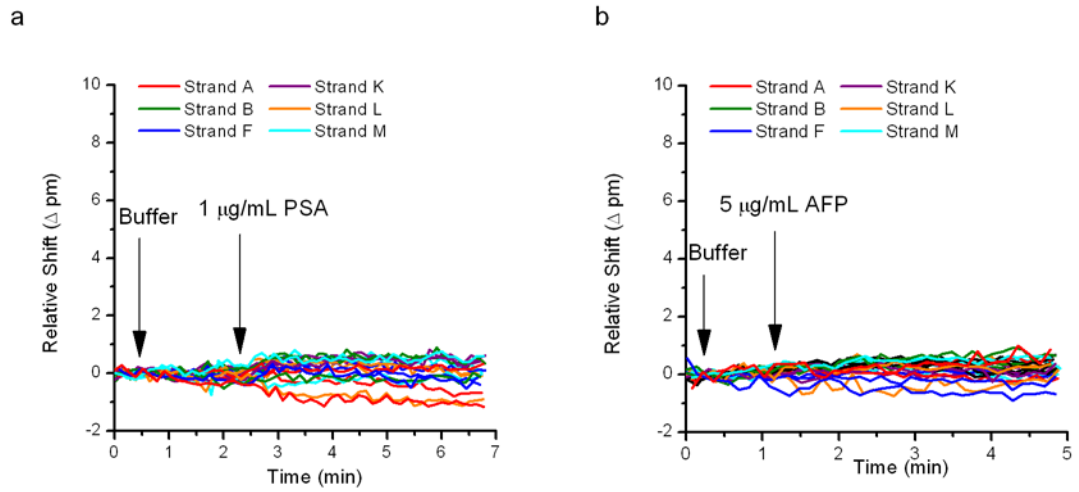

Figure S1. (a) Addition of 1 µg/mL PSA at t = 2 min. to a chip surface following several regenerations with 8M urea and functionalizations with all six anti-AFP conjugates as well as all six anti-PSA conjugates. As seen in the data, only a very small response is given to the PSA indicating a very effective regeneration with negligible carryover of capture agent. (b) The same experiment as (a) but using 5 µg/mL injected at t = 1 minute. Again, regeneration effectively eliminates any specific capture agent activity.

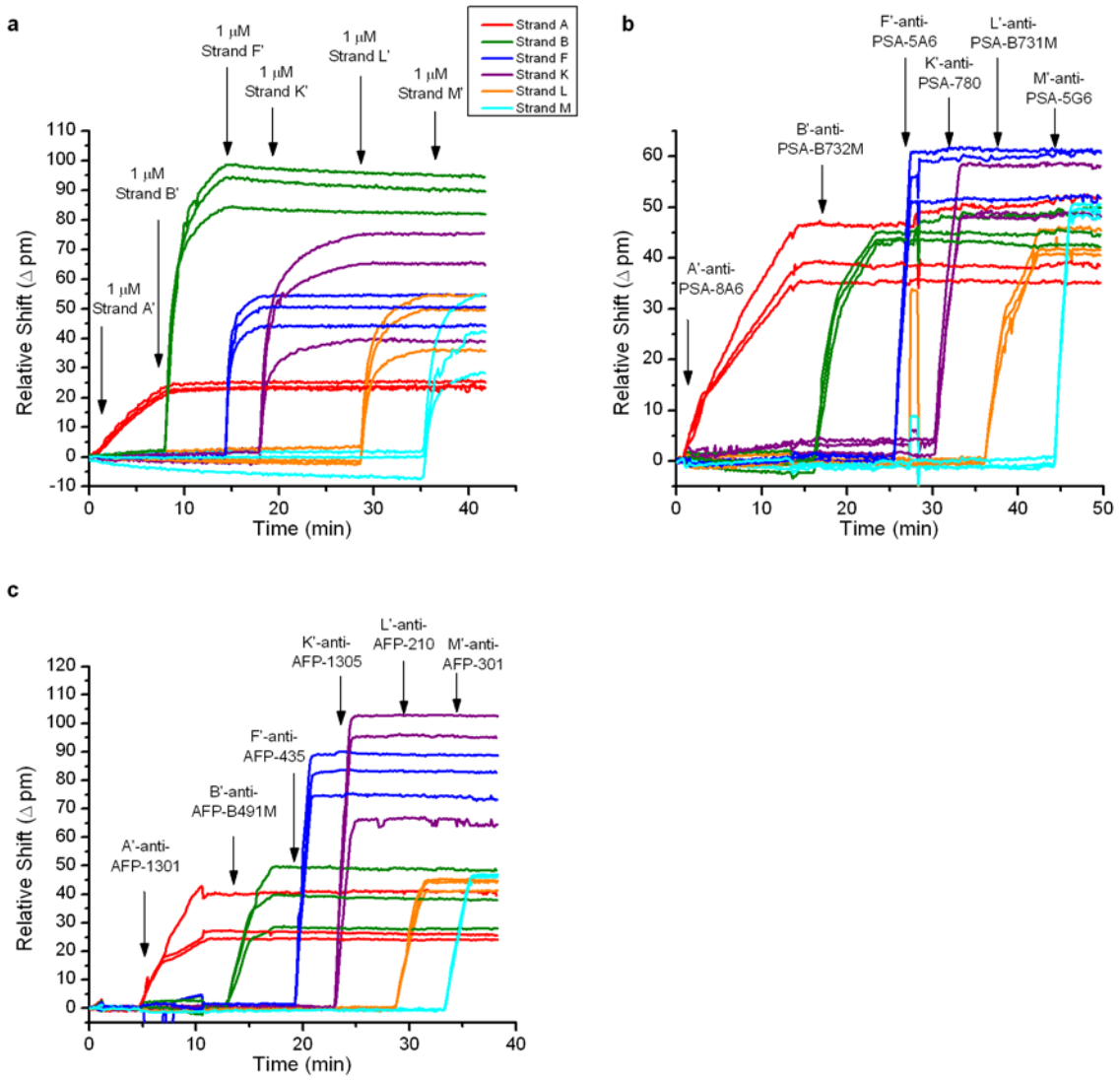

Figure S2. Real time data plots showing resonance wavelength shifts for arrays of microrings functionalized with 6 different DNA strand sequences (strands A, B, F, K, L, and M, each shown in a different color, as seen in the legend). (a) Sequential addition of 1 µM complementary DNA strands A′, B′, F′, K′, L′, M′ with no apparent cross-reactivity since only the appropriate rings respond at the time point at which the complementary strand is added. (b) Sequential addition of 6 different DNA-anti-PSA conjugates with appropriate complementary DNA. Again, only the appropriate rings respond at the time point during which the conjugate with the complementary DNA is added, so there is no apparent cross reactivity. The jump at ~27 minutes comes from an air bubble. These antibodies are loaded onto the surface following surface regeneration showing no difficulty in reloading antibody conjugates following regeneration. (c) A similar experiment as in (b) but using anti-AFP conjugates. Again, no cross reactivity is observed, and these antibodies are similarly loaded onto a surface that has experienced regeneration.

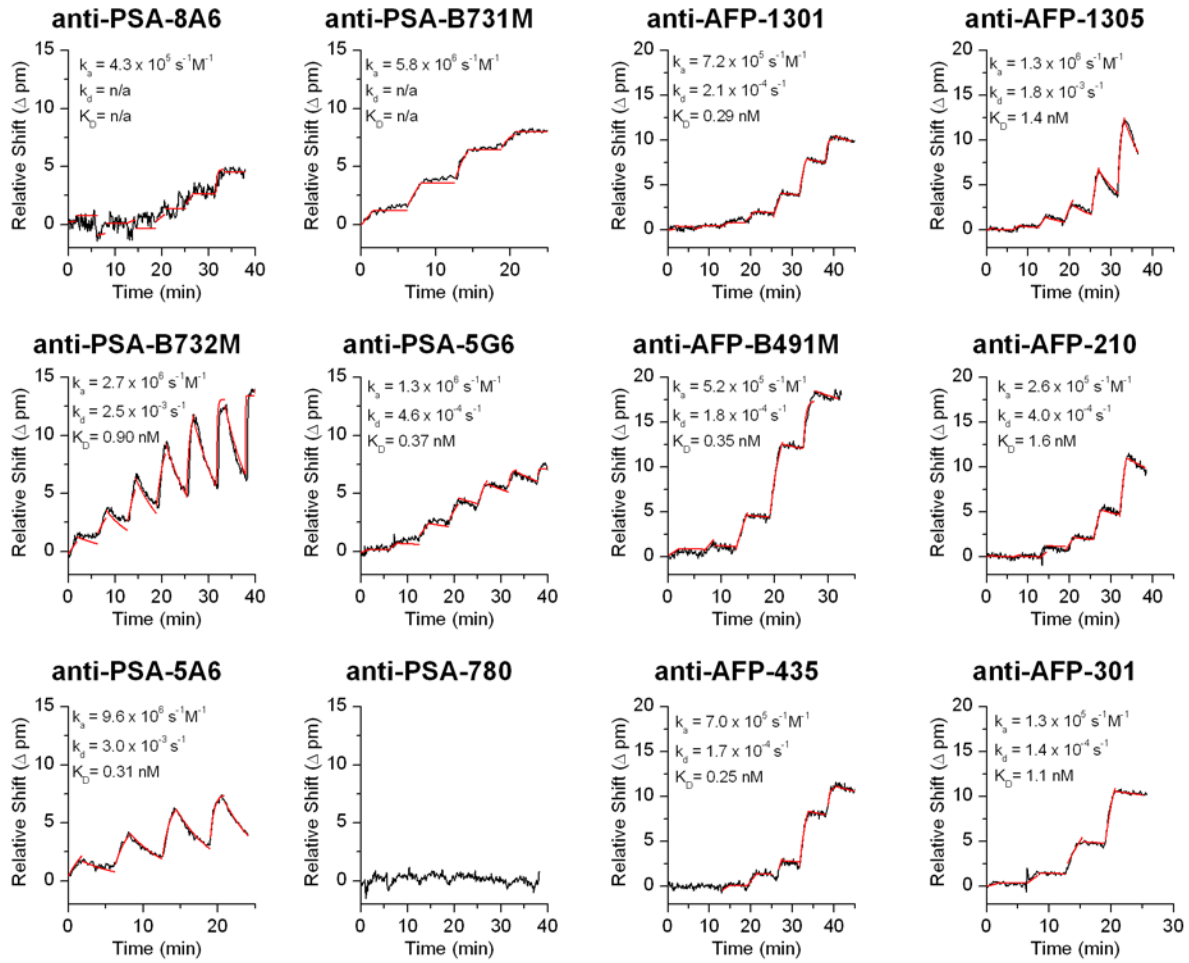

Figure S3. Real time data plots showing the kinetic titrations for each of the 12 antibodies using RAM-Fc immobilization. RAM-Fc was functionalized with DNA strand K′ similar to the other DNA-antibody conjugates and then flowed over a chip functionalized with strand K. Following addition of RAM-Fc, one of the non-modified anti-PSA or anti-AFP antibodies were flowed over the surface until 30-50 pm of antibody bound to the RAM-Fc surface. Each kinetic titration run was performed serially in a different microfluidic channel rather than in parallel within the same microfluidic channel, as done in Figures S4 and S5. The black traces indicate the real time data, and the red traces indicate the global fit via a one-to-one Langmuir binding model. In each graph, the calculated k_a, k_d, and K_D from the fit are listed, except for anti-PSA-B731M, which had too slow of a dissociation rate to accurately measure, thus "n/a" is given for those values. Also, anti-PSA-8A6 had to poor of kinetics to accurately determine k_d. Anti-PSA-780 showed almost no binding, so no fitting data for K′-anti-PSA-780 is shown. Comparing results from Figure S3 to Figure S4 and S5, most of the kinetic parameters (k_a and k_d) are within a factor of 2. The main exception is for the k_d values for anti-AFP-B491M and anti-AFP-301, which have significantly faster rates of dissociation. This can be possibly attributed to differences in binding ability of these particular antibodies when bound by RAM-Fc.

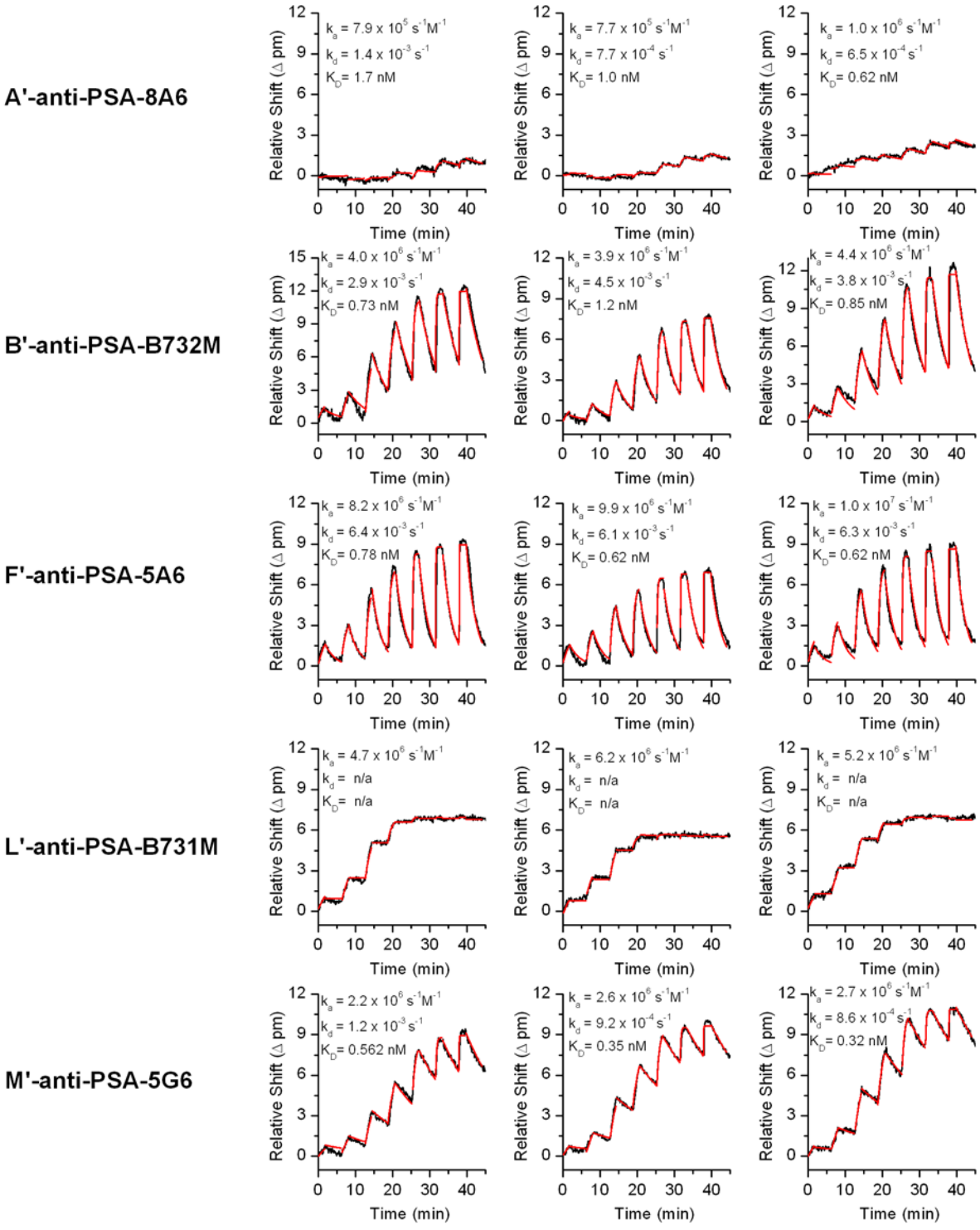

Figure S4. Real time data plots showing the kinetic titrations for 15 microring sensors (three sensors per antibody conjugate) for the anti-PSA conjugates. The black traces indicate the real time data, and the red traces indicate the global fit via a one-to-one Langmuir binding model. In each graph, the calculated k_a, k_d, and K_D from the fit are listed, except for L′-anti-PSA-B731M, which had too slow of a dissociation rate to accurately measure, thus "n/a" is given for those values. Also, anti-PSA-780 performed too poorly to generate a reliable fit, so the data for K′-anti-PSA-780 is not shown.

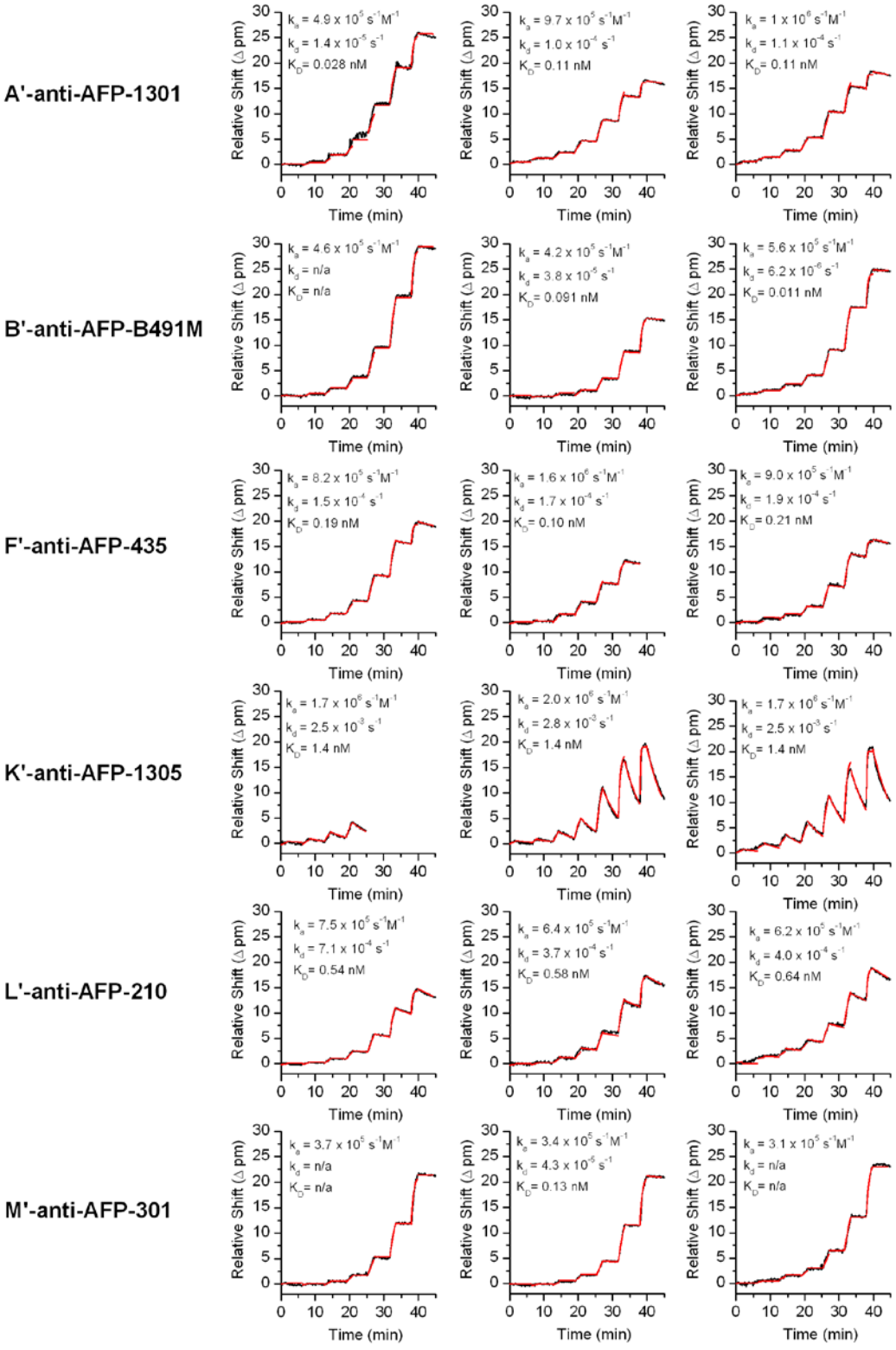

Figure S5. Real time data plots showing the kinetic titrations for 18 microring sensors (three sensors per antibody conjugate) for the anti-AFP conjugates. The black traces indicate the real time data, and the red traces indicate the global fit via a one-to-one Langmuir binding model. In each graph, the calculated k_a, k_d, and K_D from the fit are listed, except for a few of the plots, which had too slow of a dissociation rate to accurately measure, thus "n/a" is given for those values.

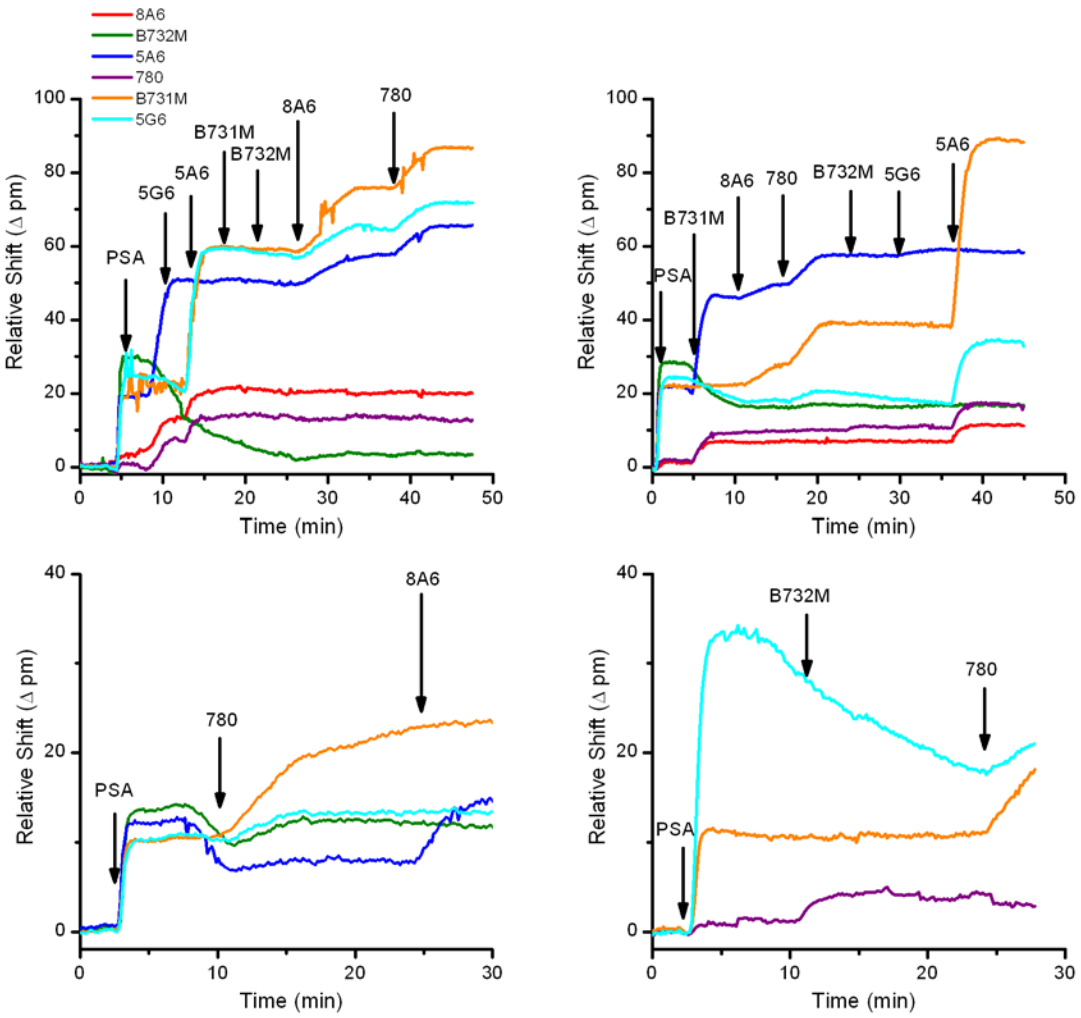

Figure S6. Real-time data for secondary antibody screening for anti-PSA antibodies. The legend in the top left graph indicates which color is associated with which anti-PSA antibody clone. After initial addition of PSA, a series of unmodified anti-PSA antibodies are added in sequence (as shown by arrows); each antibody addition is followed by a short buffer rinse before addition of the next antibody. Each graph is a different run wherein a different sequence of secondary antibodies is added; this aids in identification of which antibodies interfere with the binding of other antibodies.

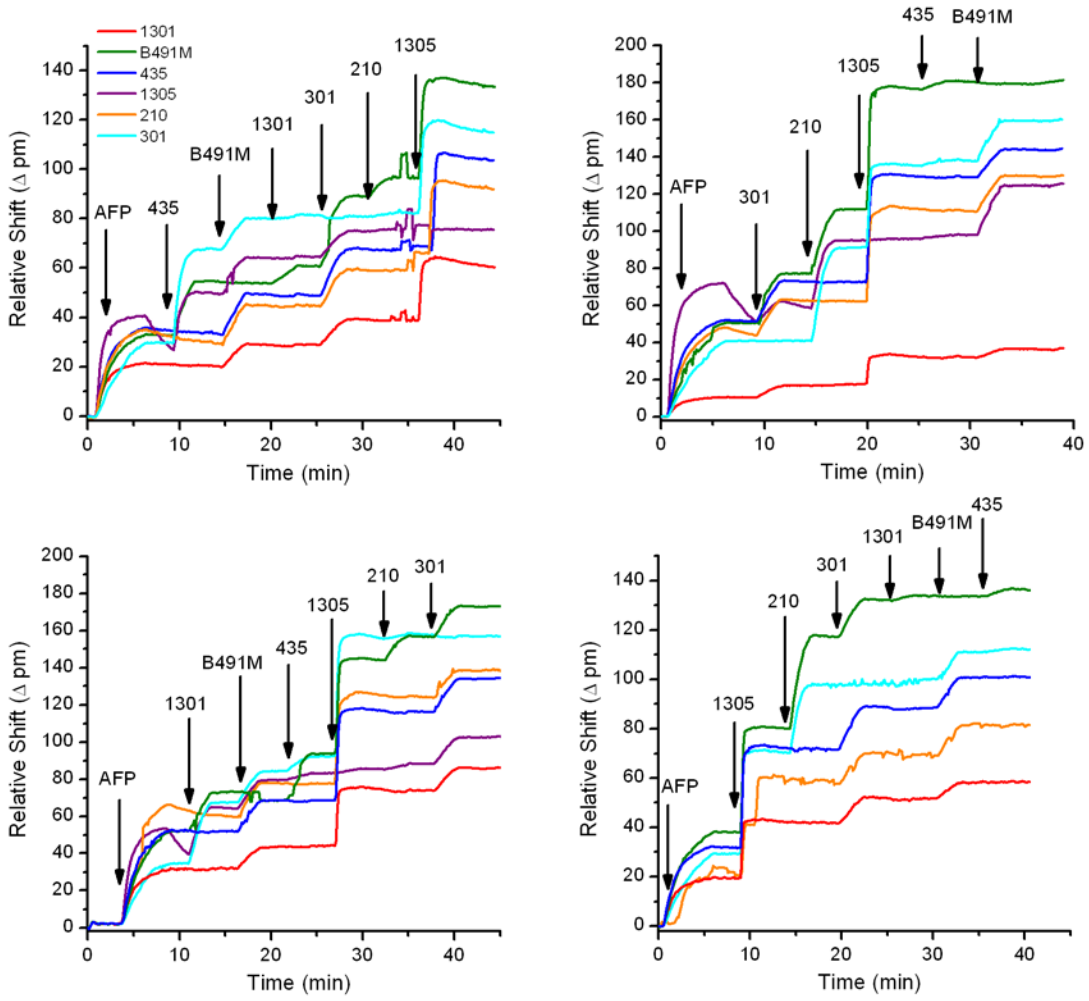

Figure S7. Real-time data for secondary antibody screening for anti-AFP antibodies. The legend in the top left graph indicates which color is associated with which anti-AFP antibody clone. After initial addition of AFP, a series of unmodified anti-AFP antibodies are added in sequence (as shown by arrows); each antibody addition is followed by a short buffer rinse before addition of the next antibody. Each graph is a different run wherein a different sequence of secondary antibodies is added; this aids in identification of which antibodies interfere with the binding of other antibodies.